

Effect of External AC Electric and Magnetic Fields on the Power Production of a Silicon Solar Cell

Hassan Fathabadi 

Abstract—One important issue is to evaluate the effect of external alternating current (ac) electric and magnetic fields on the photovoltaic (PV) power production of a PV cell. External ac electric and magnetic fields are often produced by ac power systems and devices and almost exist everywhere, which makes this issue even more crucial. This research work addresses this very important issue by presenting a novel comprehensive theoretical analysis and providing relevant experimental verifications. The outcome of this study demonstrates that the external ac electric field has no effect on the power production and open-circuit voltage of a PV cell/module, while the external ac magnetic field has a huge negative impact on the output power and open-circuit voltage of a PV cell/module. Moreover, this negative impact significantly intensifies by increasing the amount of the external ac magnetic field. Theoretical and experimental results presented in this study explicitly substantiate that to efficiently utilize PV power generation systems, locating them far from external magnetic fields is necessary.

Index Terms—Alternating current (ac) electric field, ac magnetic field, photovoltaic (PV) module, silicon PV cell.

I. INTRODUCTION

BECAUSE of environmental issues and economic considerations, there is an upward trend in developing the usage of solar energy, so that there is an ascending demand for stand-alone and grid-connected photovoltaic (PV) power generation systems. As a result, there is currently a highly concentrated attempt to enhance the power efficiency of PV cells. In this regard, the research activities mainly focus on the three items as follows. First, utilizing new or modified materials such as different cathode buffer layers [1], earth-abundant absorbers [2], and complexing agent [3] to build solar cells. Second, taking suitable peripheral elements or devices into account to improve the PV efficiency, for instance, implementing different maximum power point trackers [4]–[9] and utilizing cooling systems by using different active cooling techniques and even nanomaterials. The third item deals with evaluating the effect of the environmental parameters such as temperature on the performance of a PV cell [10]. The effect of almost all the environmental factors such as wind [11], dust [12], and mud [13] has been reported in the literature. A thorough survey of the current literature demonstrates that regarding the impact of the dc, not

alternating current (ac), electric field on silicon solar cells, the effect of the dc electric field on the open-circuit voltage of a silicon PV cell was experimentally evaluated in 2002 [14]. It was concluded that external dc electric has no effect on the open-circuit voltage of the PV cell irradiated by white light. Several research works have been performed pertaining to the impact of the dc, not ac, magnetic field on a silicon PV cell, which are discussed as follows. The impact of an external dc magnetic field on the open-circuit voltage of a CdS/CuInSe₂ PV cell was experimentally evaluated by applying a dc magnetic field to the PV cell [14]. The intensity of the magnetic field was changed from 0.003 to 0.079 T, and it was concluded that the dc magnetic field has no effect on the open-circuit voltage of the PV cell irradiated by white light. In the second research performed by the same author, it was concluded that the open-circuit voltage decreases by intensifying the magnetic field [15]. In the third research, the effect of a dc magnetic field on a silicon solar cell was theoretically assessed by considering a three-dimensional model of the PV cell [16]. The authors theoretically concluded that the output power of the PV cell decreases when the external dc magnetic field is intensified. In the last research, a theoretical study concerning the impact of the dc magnetic field on a bifacial silicon solar cell was performed by modeling the cell [17]. It was theoretically concluded that the maximum output power of the PV cell declines with the increase in the magnetic field.

The survey also demonstrates that there is not any research regarding the effect of external ac electric and magnetic fields on the output power of a PV cell/module. This study addresses this issue by presenting not only a novel comprehensive theoretical analysis but also related experimental verifications. The rest of this paper is organized as follows. The effect of an external electric field is theoretically analyzed in Section II. Similarly, the impact of an external magnetic field is evaluated in Section III. Experimental verifications are given in Section IV, and the paper is concluded in Section V.

II. EVALUATING THE INFLUENCE OF THE EXTERNAL ELECTRIC FIELD ON A SILICON PV CELL

The structure of a silicon PV cell is shown in detail in Fig. 1. In the p–n junction of the PV cell, electrons, which are majority carrier in the emitter (n-type semiconductor), move from the emitter toward the base (p-type semiconductor), so positive ion cores appear in the emitter. Similarly, holes, which are majority carrier in the base, move from the base toward the emitter, so negative ion cores occur in the base. The two exposed ionic areas form a depletion region and produce an electric field (\vec{E})

Manuscript received February 22, 2018; revised May 22, 2018 and July 4, 2018; accepted July 17, 2018.

The author is with the National Technical University of Athens, Athens 10682, Greece (e-mail: h4477@hotmail.com).

Color versions of one or more of the figures in this paper are available online at <http://ieeexplore.ieee.org>.

Digital Object Identifier 10.1109/JPHOTOV.2018.2860946

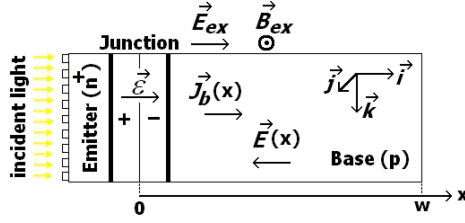


Fig. 1. Structure of a silicon solar cell.

at the junction ($x = 0$) called “junction electric field” that its direction is from the emitter to the base, as shown in Fig. 1. Irradiating the PV cell by light generates electron–hole pairs when the energy of the incident photon becomes more than that of the band gap energy. Electrons in the base and holes in the emitter are metastable and exist for a length of time called “minority carrier lifetime” before they recombine. But, if a light-generated minority carrier reaches the p–n junction, it is immediately swept across the junction by the junction electric field (\vec{E}) and participates in the production of photocurrent. Collecting light-generated minority carriers by the p–n junction causes a movement of electrons to the emitter and holes to the base, so the photocurrent is produced along the silicon PV cell. The photocurrent density in the base does not remain constant and decreases along the base because of electron–hole recombination, so the photocurrent density in the base is a function of the distance from the junction (x) and is represented by $\vec{J}_b(x)$ in Fig. 1. The relationship between the magnitudes of the junction electric field and photocurrent density at the junction ($x = 0$) is expressed as [18]

$$|\vec{E}| = \frac{|\vec{J}_b(0)|}{q(n\mu_n + p\mu_p)} \quad (1)$$

where n is the density of light-generated electrons in the base, μ_n is the electron’s intrinsic mobility, p is the density of light-generated holes in the emitter, μ_p is the hole’s mobility, and q is the elementary charge, i.e., $q = 1.602 \times 10^{-19}$ C. The photocurrent density at the junction is obtained from (1) as

$$|\vec{J}_b(0)| = q(n\mu_n + p\mu_p) |\vec{E}|. \quad (2)$$

Applying an external electric field (\vec{E}_{ex}) in the direction of the junction electric field such as that shown in Fig. 1 modifies (2) as

$$|\vec{J}_b(0)| = q(n\mu_n + p\mu_p) (|\vec{E}| + |\vec{E}_{ex}|). \quad (3)$$

Thus, the photocurrent density increases, which results in enhancing the power production of the PV cell too. Similarly, the photocurrent density, and hence, PV power decreases when the external electric field points in the direction opposite to the junction electric field because in this case the photocurrent density at the junction is obtained as

$$|\vec{J}_b(0)| = q(n\mu_n + p\mu_p) (|\vec{E}| - |\vec{E}_{ex}|). \quad (4)$$

An external ac electric field originating from an ac voltage such as that produced by an HV power transmission line is

sinusoidal. At positive half-cycle, it points in the direction of the junction electric field, while at the negative half-cycle, it points in the opposite direction. This means that an external ac electric field has no impact on the photocurrent density, and therefore, on the PV cell’s output power because the photocurrent density over one complete cycle is found using (3) as

$$\begin{aligned} |\vec{J}_b(0)| &= \int_0^T q(n\mu_n + p\mu_p) [|\vec{E}| + E_m \sin(\omega t)] dt \\ &= q(n\mu_n + p\mu_p) |\vec{E}| + q(n\mu_n + p\mu_p) \int_0^T E_m \sin(\omega t) dt \\ &= q(n\mu_n + p\mu_p) |\vec{E}| \end{aligned} \quad (5)$$

where E_m and ω are, respectively, the magnitude and angular frequency of the external ac electric field. Equation (5) explicitly demonstrates that the photocurrent density, and as a consequence, the PV power production and open-circuit voltage of the silicon PV cell do not depend on the external ac electric field. Thus, it is concluded that an external ac electric field has no impact on the power production and open-circuit voltage of a PV cell as well as a PV module.

III. EVALUATING THE INFLUENCE OF THE EXTERNAL MAGNETIC FIELD ON A SILICON PV CELL

By applying an external magnetic field to a PV cell like that shown in Fig. 1, the minority carriers (electrons) coming from the base toward the p–n junction deviate from their path, and a reduction in their effective mobility occurs. Similarly, the minority carriers (holes) coming from the emitter toward the junction deviate from their trajectory, which results in a reduction in their effective mobility. As a consequence, the photocurrent density in the base deviates from its original path along the x -axis. In Fig. 1, the electrons in the base and the holes in the emitter turn to, respectively, up and down. When an external ac magnetic field such as that produced by an HV power transmission is applied, the only difference is that the electrons in the base turn to up at the positive half-cycle and turn to down at the negative half-cycle. Under this condition, the holes in the emitter turn to the direction opposite to that of the electrons in the base. Thus, the impact of an ac magnetic field on the PV cell is similar to that of a constant magnetic field. They both decrease the output power of the PV cell by reducing the effective mobility of the minority carriers participating in photocurrent production. This point can be also formulized as follows. The photocurrent density in the base is expressed by using the transportation phenomena equation as [19]

$$\vec{J}_b(x) = qD_n \vec{\nabla} \delta(x) + q\mu_n \delta(x) \vec{E}(x) \quad (6)$$

where D_n is the electron’s intrinsic diffusion coefficient, $\delta(x)$ is the excess minority carrier density in the base, and $\vec{E}(x)$ is the electric field originating from carrier concentration gradient along the base that its magnitude is given as [20]

$$|\vec{E}(x)| = \frac{D_p - D_n}{\mu_p + \mu_n} \frac{1}{\delta(x)} \frac{d\delta(x)}{dx}. \quad (7)$$

Equation (7) is used when a solar cell is illuminated with an intense light concentration more than 50 suns resulting under a very high injection condition. In Fig. 1, in the absence of the external magnetic field (\vec{B}_{ex}), there is no deviation in the electrons' trajectory, and the photocurrent density in the base is in the direction of the vector \vec{i} , so (6) can be rewritten as

$$\left| \vec{J}_b(x) \right| \vec{i} = qD_n \frac{d\delta(x)}{dx} \vec{i} - q\mu_n \delta(x) \left| \vec{E}(x) \right| \vec{i}. \quad (8)$$

By substituting $|\vec{E}(x)|$ from (7) into (8), the magnitude of the photocurrent density in the base in the absence of the external magnetic field is found as

$$\left| \vec{J}_b(x) \right| = q \left[\frac{\mu_p D_n - \mu_n D_p + 2\mu_n D_n}{\mu_p + \mu_n} \right] \frac{d\delta(x)}{dx}. \quad (9)$$

Under the influence of the external magnetic field (\vec{B}_{ex}) shown in Fig. 1, the transportation phenomena equation [see (6)] giving the photocurrent density in the base changes as follows:

$$\vec{J}_b(x) = qD_n \vec{\nabla} \delta(x) + q\mu_n \delta(x) \vec{E}(x) - \mu_n \vec{J}_b(x) \times \vec{B}_{\text{ex}}. \quad (10)$$

As mentioned before, the photocurrent density in the base deviates from its original path along the x -axis when the external magnetic field is applied. By substituting $|\vec{E}(x)|$ from (7) into (10), the magnitude of the photocurrent density in the base along the x -axis in the presence of the external magnetic field is obtained as

$$\left| \vec{J}_{bx}(x) \right| = q \left[\frac{\mu_p D_n - \mu_n D_p + 2\mu_n D_n}{\left(1 + \mu_n^2 |\vec{B}_{\text{ex}}|^2 \right)^{0.5} (\mu_p + \mu_n)} \right] \frac{d\delta(x)}{dx}. \quad (11)$$

Comparing (11) giving the photocurrent density in the presence of the external magnetic field with (9) expressing the photocurrent density in the absence of the external magnetic field explicitly demonstrates that by applying the external magnetic field, the photocurrent density decreases by the factor $\frac{1}{(1 + \mu_n^2 |\vec{B}_{\text{ex}}|^2)^{0.5}}$, and hence, the power production declines too.

When the PV cell is irradiated with a normal light (not an intense light), for example, one sun or less, the gradient of the minority carrier density along the base becomes small, i.e., $\frac{d\delta(x)}{dx} \rightarrow 0$, but in fact it is not zero, i.e., $\frac{d\delta(x)}{dx} \neq 0$. As a consequence, the electric field originating from carrier concentration gradient along the base ($\vec{E}(x)$) becomes small, i.e., $|\vec{E}(x)| \rightarrow 0$, but $|\vec{E}(x)| \neq 0$. Thus, (9) and (11) expressing the photocurrent density in the base should be even satisfied when the PV cell is illuminated with a moderate light (low-level injection) resulting in a decrease of the photocurrent density with the increase of the external magnetic field.

Using the single-diode model, the open-circuit voltage of the PV cell is expressed as

$$A \left| \vec{J}_{bx}(x) \right| = \frac{V_{\text{oc}}}{R_p} + I_o \left[\exp \left(\frac{qV_{\text{oc}}}{nK_B T} \right) - 1 \right] \quad (12)$$

where A is the cross-sectional area of the junction, K_B is the Boltzmann constant, I_o is the saturation current of the equivalent diode, and V_{oc} , T , R_p , and n are, respectively, the open-circuit voltage, absolute temperature, shunt resistance, and ideality factor of the PV cell. The right-hand side of (12) can be estimated as

$$A \left| \vec{J}_{bx}(x) \right| \approx V_{\text{oc}} \left(\frac{1}{R_p} + \frac{qI_o}{nK_B T} \right). \quad (13)$$

By substituting $|\vec{J}_{bx}(x)|$ from (11) into (13), the open-circuit voltage under the influence of the external magnetic field is obtained as

$$V_{\text{oc}} \approx \left[\frac{Aq(\mu_p D_n - \mu_n D_p + 2\mu_n D_n)}{\left(\frac{1}{R_p} + \frac{qI_o}{nK_B T} \right) \left(1 + \mu_n^2 |\vec{B}_{\text{ex}}|^2 \right)^{0.5} (\mu_p + \mu_n)} \right] \frac{d\delta(x)}{dx}. \quad (14)$$

It is reminded that R_p slightly increases with the increase in the magnetic field, so (14) clearly demonstrates that increase or decrease in the open-circuit voltage of the PV cell depends on the factor $\left(\frac{1}{R_p} + \frac{qI_o}{nK_B T} \right) (1 + \mu_n^2 |\vec{B}_{\text{ex}}|^2)^{0.5}$ in which R_p and $|\vec{B}_{\text{ex}}|$ both increase.

The complex mobility of the excess minority carriers (electrons) in the base under frequency modulation and magnetic field is expressed as [21]

$$\mu_n^* = \frac{\mu_n [1 + \tau_n^2 (\omega_c^2 - \omega^2) + j\omega\tau_n (\tau_n^2 (\omega_c^2 - \omega^2) - 1)]}{4\omega^2 \tau_n^2 + [1 + \tau_n^2 (\omega_c^2 - \omega^2)]^2} \quad (15)$$

where τ_n is the average lifetime of electrons in the base, $\omega = 2\pi f$ is the angular frequency, $\omega_c = \frac{q|\vec{B}_{\text{ex}}|}{m_n}$ is the cyclotron frequency, and m_n is the effective mass of electron. The relationship between the complex diffusion coefficient of the excess minority carriers in the base (D_n^*) and μ_n^* is expressed as

$$\frac{D_n^*}{\mu_n^*} = \frac{K_B T}{q}. \quad (16)$$

By substituting μ_n^* from (15) into (16), the complex diffusion coefficient is obtained as

$$D_n^* = \frac{D_n [1 + \tau_n^2 (\omega_c^2 - \omega^2) + j\omega\tau_n (\tau_n^2 (\omega_c^2 - \omega^2) - 1)]}{4\omega^2 \tau_n^2 + [1 + \tau_n^2 (\omega_c^2 - \omega^2)]^2}. \quad (17)$$

Equation (17) demonstrates that resonance picks occur at $f = f_c = \frac{\omega_c}{2\pi}$. In practice $f_c > 10^4 \text{ Hz}$ [21], so the resonance picks occur in the frequency range of $f > 10^4 \text{ Hz}$, which does not include low-frequency (50/60 Hz) magnetic fields produced by ac power systems and devices.

IV. EXPERIMENTAL VERIFICATIONS

In this section, experimental verifications are presented to validate the theoretical result obtained in the previous sections. A polycrystalline PV module STP300-24/Ve made by Suntech Power Holdings Co. has been utilized to provide experimental verifications. The electrical characteristics of the PV module STP300-24/Ve under the standard test condition (STC), which

TABLE I
ELECTRICAL CHARACTERISTICS OF THE POLYCRYSTALLINE
PV MODULE STP300-24/VE UNDER STC

Current at MPP (I_{pv-mpp})	8.36 A
Voltage at MPP (V_{pv-mpp})	35.9 V
Output power at MPP (P_{pv-mpp})	300 W
Short-circuit current (I_{sc})	8.83 A
Open-circuit voltage (V_{oc})	44.5 V

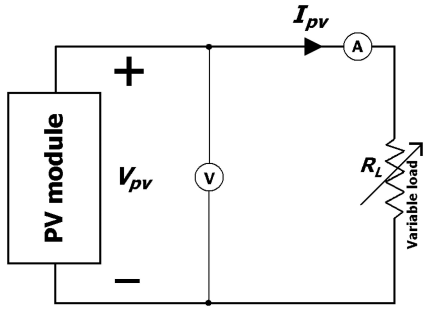


Fig. 2. Electrical set-up for measuring the output voltage, current, and power of the PV module.

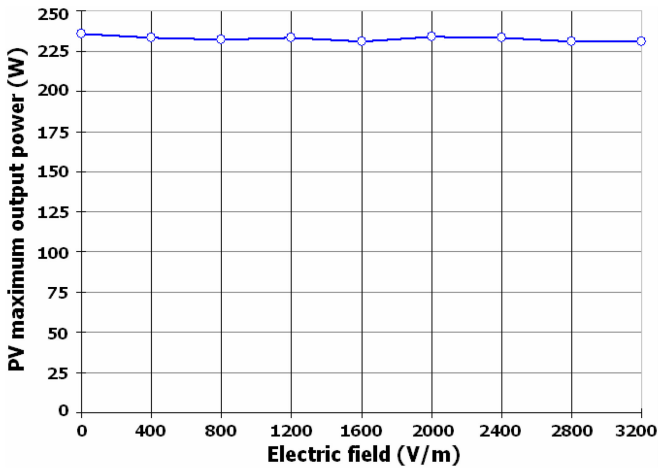


Fig. 3. PV maximum output power versus the external ac electric field: $G = 821 \text{ Wm}^{-2}$ and $T = 26^\circ\text{C}$.

refers to solar irradiance (G) of 1000 Wm^{-2} , module temperature (T) of 25°C , and air mass of 1.5, are reported in Table I. The electrical set-up shown in Fig. 2 was assembled to measure the output voltage (V_{pv}) and output current (I_{pv}), and hence to calculate the output power ($P_{pv} = V_{pv} I_{pv}$) of the PV module. Two experiments were performed under conditions that solar irradiance and the PV module temperature were measured at, respectively, 821 Wm^{-2} and 26°C . In the first test, an external ac electric field was produced by utilizing two plates and supplying an ac voltage to the plates. The magnitude of the ac electric field produced was changed by varying the magnitude of the ac voltage, and maximum output power produced by the PV module was measured point by point for each amount of

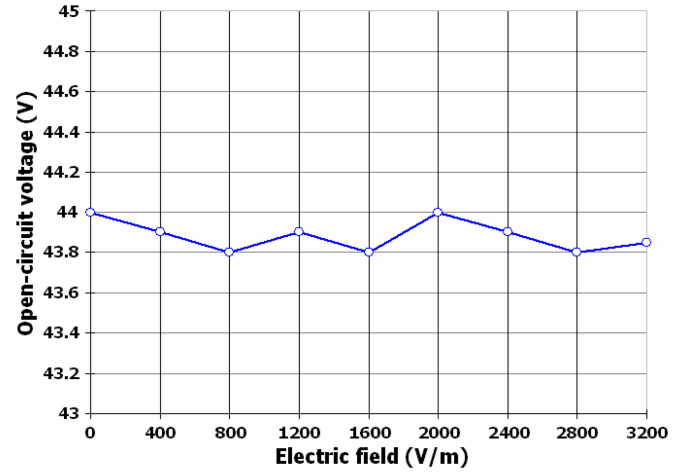


Fig. 4. Open-circuit voltage of the PV module versus the external ac electric field: $G = 821 \text{ Wm}^{-2}$ and $T = 26^\circ\text{C}$.

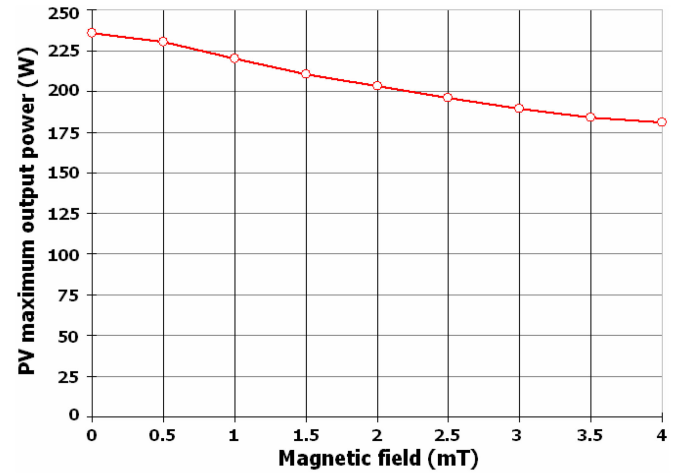


Fig. 5. PV maximum output power versus the external ac magnetic field: $G = 821 \text{ Wm}^{-2}$ and $T = 26^\circ\text{C}$.

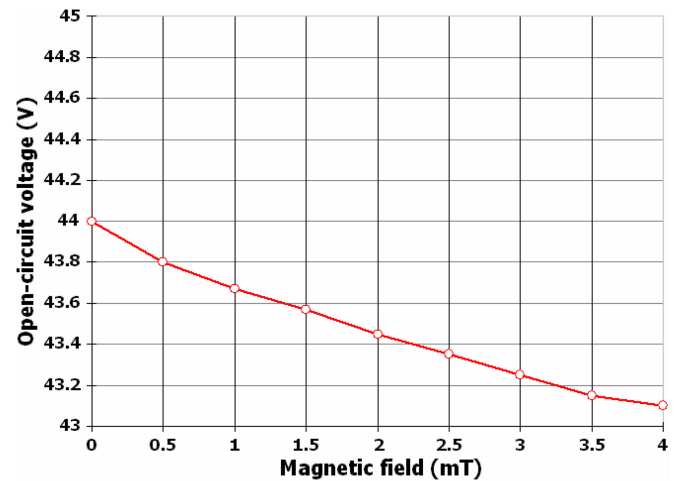


Fig. 6. Open-circuit voltage of the PV module versus the external ac magnetic field: $G = 821 \text{ Wm}^{-2}$ and $T = 26^\circ\text{C}$.

the electric field. The maximum output power measured versus the amount of the external ac electric field is shown as a curve in Fig. 3. The experimental measurements shown in Fig. 3 explicitly demonstrate that the ac electric field has no effect on the power production of the PV module. This point explicitly verifies the outcome of the theoretical analysis performed in Section II. Also, the open-circuit voltage of the PV module versus the amount of the external ac electric field is shown in Fig. 4, which verifies this fact that the external ac electric field has no impact on the open-circuit voltage of the PV module too.

In the second experiment, an external ac magnetic field was produced by utilizing a solenoid with an inductance of 11.3 mH. The amount of the magnetic field was changed by varying the magnitude of the ac electric current supplied to the solenoid. The maximum output power of the PV module was measured for each amount of the external magnetic field. The measured maximum output power versus the amount of the external magnetic field is shown as a curve in Fig. 5. The experimental curve demonstrates that the maximum output power of the PV module significantly decreases when the amount of the external ac magnetic field increases. This point explicitly verifies the outcome of the theoretical analysis performed in Section III. The open-circuit voltage of the PV module versus the amount of the external ac magnetic field is also shown in Fig. 6, which explicitly verifies the reduction in the open-circuit voltage of the PV module caused by the external ac magnetic field.

V. CONCLUSION

In this study, a novel comprehensive theoretical analysis was presented to show the effect of ac electric and magnetic fields on the power production of a PV cell/module. The relevant experimental verifications were given, and it was demonstrated that the external ac electric field has no effect on the output power and open-circuit voltage of the PV cell/module, while the external ac magnetic field has a huge negative impact on the output power and open-circuit voltage. Furthermore, this negative impact considerably intensifies by enhancing the amount of the external ac magnetic field. The results obtained in this study can be widely used by readers to position PV modules/panels in suitable locations far from external magnetic fields.

REFERENCES

- [1] G. Lastra *et al.*, "High-performance inverted polymer solar cells: Study and analysis of different cathode buffer layers," *IEEE J. Photovolt.*, vol. 8, no. 2, pp. 505–511, Mar. 2018.
- [2] S. Sinha, D. K. Nandi, S. H. Kim, and J. Heo, "Atomic-layer-deposited buffer layers for thin film solar cells using earth-abundant absorber materials: A review," *Sol. Energy Mater. Sol. Cells*, vol. 176, pp. 49–68, 2018.
- [3] T. Hildebrandt *et al.*, "Use of a new organic complexing and buffer agent for Zn(S,O) deposition for high-efficiency Cu(In,Ga)Se₂-based solar cells," *IEEE J. Photovolt.*, vol. 8, no. 1, pp. 266–271, Mar. 2018.
- [4] H. Fathabadi, "Novel fast and high accuracy maximum power point tracking method for hybrid photovoltaic/fuel cell energy conversion systems," *Renew. Energy*, vol. 106, pp. 232–242, 2017.
- [5] H. Fathabadi, "Novel high accurate sensorless dual-axis solar tracking system controlled by maximum power point tracking unit of photovoltaic systems," *Appl. Energy*, vol. 173, pp. 448–459, 2016.
- [6] H. Fathabadi, "Novel fast dynamic MPPT (maximum power point tracking) technique with the capability of very high accurate power tracking," *Energy*, vol. 94, pp. 466–475, 2016.
- [7] H. Fathabadi, "Novel highly accurate universal maximum power point tracker for maximum power extraction from hybrid fuel cell/photovoltaic/wind power generation systems," *Energy*, vol. 116, pp. 402–416, 2016.
- [8] H. Fathabadi, "Novel all-purpose high-power matching device for energy conversion applications," *Energy Convers. Manage.*, vol. 149, pp. 121–128, 2017.
- [9] H. Fathabadi, "Novel high-efficient large-scale stand-alone solar/wind hybrid power source equipped with battery bank used as storage device," *J. Energy Storage*, vol. 17, pp. 485–495, 2018.
- [10] A. M. Elbreki, M. A. Alghoul, K. Sopian, and T. Hussein, "Towards adopting passive heat dissipation approaches for temperature regulation of PV module as a sustainable solution," *Renew. Sustain. Energy Rev.*, vol. 69, pp. 961–1017, 2017.
- [11] J. K. Kaldellis, M. Kapsali, and M. A. Kavadias, "Temperature and wind speed impact on the efficiency of PV installations. Experience obtained from outdoor measurements in Greece," *Renew. Energy*, vol. 66, pp. 612–624, 2014.
- [12] J. Tanesab, D. Parlevliet, J. Whale, and T. Urmee, "Seasonal effect of dust on the degradation of PV modules performance deployed in different climate areas," *Renew. Energy*, vol. 111, pp. 105–115, 2017.
- [13] B. S. Yilbas, H. Ali, F. Al-Sulaiman, and H. Al-Qahtani, "Effect of mud drying temperature on surface characteristics of a polycarbonate PV protective cover," *Sol. Energy*, vol. 143, pp. 63–72, 2017.
- [14] S. Erel, "The effect of electric and magnetic fields on the operation of a photovoltaic cell," *Sol. Energy Mater. Sol. Cells*, vol. 71, pp. 273–280, 2002.
- [15] S. Erel, "Comparing the behaviors of some typical solar cells under external effects," *TEKNOLOJI*, vol. 11, no. 3, pp. 233–237, 2008.
- [16] A. Dieng, N. Thiam, A. Thiam, A. S. Maiga, and G. Sissoko, "Magnetic field effect on the electrical parameters of a polycrystalline silicon solar cell," *Res. J. Appl. Sci. Eng. Technol.*, vol. 3, no. 7, pp. 602–611, 2011.
- [17] I. Zerbo *et al.*, "External magnetic field effect on bifacial silicon solar cell's electric power and conversion efficiency," *Turkish J. Phys.*, vol. 39, pp. 288–294, 2015.
- [18] A. L. Fahrenbruch and R. H. Bube, *Fundamentals of Solar Cells*. New York, NY, USA: Academic, 1983.
- [19] Y. Betser, D. Ritter, G. Bahir, S. Cohen, and J. Sperling, "Measurement of the minority carrier mobility in the base of heterojunction bipolar transistor using magneto-transport method," *Appl. Phys. Lett.*, vol. 67, no. 13, pp. 1883–1884, 1995.
- [20] F. Pelanchon, C. Sudre, and Y. Moreau, "Solar cells under intense light concentration: numerical and analytical approaches," in *Proc. 11th Eur. Photovolt. Sol. Energy Conf.*, Montreux, France, 1992, pp. 265–267.
- [21] A. Diao *et al.*, "Diffusion coefficient in silicon solar cell with applied magnetic field and under frequency: Electric equivalent circuits," *World J. Condens. Matter Phys.*, vol. 4, pp. 84–92, 2014.



Hassan Fathabadi was born in Tehran, Iran, in 1969. He received the B.S., M.S., and Ph.D. degrees in electrical engineering from Tehran Polytechnic University, Tehran, Iran, in 1992, 1997, and 2002, respectively.

From 2009 to 2012, he was a Postdoctoral Researcher with the National Technical University of Athens, Athens, Greece, where he is currently an Associate Professor. He is the sole author of more than 70 papers published in high-ranking ISI journals and 25 inventions. His research interests include power

electronics, microelectronics, control, mechatronics, energy conversion, and power systems.